# Using the spatial pattern of water isotope ratios to understand peatland hydrology: Examples from Northeast China and a model-based interpretive framework

Zhengyu Xia[1,2], Yuexin Liu[1,2], Can Zhang[3], Yuefeng Li[1,2], Zicheng Yu[1,2,4]

[1] MOE Key Laboratory of Geographical Processes and Ecological Security in Changbai Mountains, School of Geographical Sciences, Northeast Normal University, Changchun, China
[2] State Environmental Protection Key Laboratory of Wetland Ecology and Vegetation Restoration, Northeast Normal University, Changchun, China
[3] State Key Laboratory of Lake Science and Environment, Nanjing Institute of Geography and Limnology, Chinese Academy of Sciences, Nanjing, China
[4] State Key Laboratory of Black Soil Conservation and Utilization, Northeast Institute of Geography and Agroecology, Chinese Academy of Sciences, Changchun, China

## SUMMARY

Hydrology is the fundamental control of peatland ecosystems. The spatial pattern of isotopic variability in peatland water provides insights into the site-scale heterogeneity of water sources, turnover and flow patterns. However, we still lack comprehensive documentation of spatial isotope datasets across different peatland types and climates, and no study has presented an interpretative framework for such spatial data or related them to quantitative models of isotopic fractionation. Here we investigate the spatial distribution of isotope ratios in water at the peatland surface within temperate peatlands of three different types (sloping poor fen, drainage-affected poor fen on a flat platform, steeply sloping bog with strong pool patterning) in Northeast China and develop a mechanistic model of isotopic fractionation for a generalised understanding of relevant mechanisms. Our data show an evaporation-induced increasing trend in peatland water $\delta^{18}O$ towards the downslope direction in the sloping poor fen. This pattern can be reproduced by the model simulation but is not observed in the drainage-affected poor fen or in the patterned bog. The latter two sites show isotopic heterogeneities that directly indicate poor surface water connectivity due to topographic, hydraulic and hydrological factors, as supported by the model sensitivity analysis and constraints from river isotope data. Additionally, all three sites have notably narrow ranges of variability in peatland water $\delta^{18}O$ compared to previously investigated European and North American peatlands. This may result from the high transpiration fraction of herbaceous vegetation and accelerated turnover of the surface water reservoir under a wet monsoon climate, which together prevent the development of strongly enriched isotopic signatures in regional peatlands. This study underscores the potential for using the spatial distribution of water isotope ratios as a simple and efficient method to distinguish surface hydrology among different hydrogenetic types of peatlands, with scope for making quantitative inferences by developing isotope-based hydrological models.

**KEY WORDS:** evapotranspiration partitioning, hydrological processes, mechanistic modelling, temperate peatlands, water isotope tracers

## INTRODUCTION

Peatlands are a special type of wetlands where plant production exceeds decomposition and fluvial export, allowing the accumulation of peat over long timescales. According to the new United Nations Environment Programme report, peatlands occupy only 3–4 % of the total land area (approximately 35–45 % of the total wetland area, Fluet-Chouinard *et al.* 2023) but store one-third of global soil carbon, totalling 450–650 Gt (UNEP 2022). Besides the tremendous value of carbon stocks, peatlands provide a range of benefits and services for humans similar to those recognised for wetlands in general. These include water conservation, water purification and flood control, with high biodiversity native to rare biota (Rydin & Jeglum 2013, UNEP 2022).

Hydrology is considered the single most important condition that controls the pattern, process and function of peatland ecosystems (Rydin & Jeglum 2013). Peatlands are commonly classified into two types based on their source of water, i.e., nutrient-poor bogs fed by precipitation and nutrient-rich fens fed by groundwater or surface water inflow. They can also be classified based on the role of water in peat formation, known as hydrogenetic types. Joosten & Clarke (2002) defined many hydrogenetic types in their classification scheme, considering features including water source, amount of water supply, slope, water storage capacity and effect on landscape water storage. Moreover, peatland hydrology has complex interactions with underlying terrain, climate, vegetation and peat accumulation, which together produce diverse features of surface morphology and patterning at various spatial scales, from microtopographical units (e.g., hummocks, pools) to landscape structures (e.g., raised bogs, patterned fens) (Rydin & Jeglum 2013). Peatland hydrologists are generally interested in determining the water budget (Price & Maloney 1994, Evans *et al.* 1999), water flow (Devito *et al.* 1997, Fraser *et al.* 2001, van Loon *et al.* 2009) and water quality (Vitt *et al.* 1995, Prévost *et al.* 1999) of peatlands using field and laboratory measurements, which can be expensive, time-consuming and uncertain when it comes to characterising spatial heterogeneity (Beckwith *et al.* 2003, Holden 2005, Graham *et al.* 2016, Arsenault *et al.* 2019).

Stable isotopes of natural waters ($\delta^2H$ and $\delta^{18}O$) are conservative tracers that are useful for investigating peatland hydrology. Three specific approaches can be summarised from the literature. The first infers the origin of water based on apparent similarities in measured δ-values between peatland water and potential source waters such as precipitation, groundwater and surface water (Chapman *et al.* 2003, Zanazzi & Mora 2005, Daley *et al.* 2010, Keimowitz *et al.* 2013, Levy *et al.* 2014, Shi *et al.* 2019). This source water information is vital for the classification of peatlands (Keimowitz *et al.* 2013). The second approach investigates peatland water balance and turnover based on the isotopic deviation from the source water (Nichols *et al.* 2010, Bootsma *et al.* 2019, Muhic *et al.* 2023). Water primarily exits peatlands as evapotranspiration and groundwater or surface water outflow. Among these effluxes, only evaporation leads to isotopic fractionation, with more-enriched δ-values in peatland water indicating a greater contribution of evaporation to the water balance and presumably a slower water turnover or longer residence time, as frequently shown in studies of lake water systems (Gibson & Edwards 2002, Gibson *et al.* 2016). The third approach investigates the heterogeneity of water source and turnover characteristics based on the spatial (and/or vertical) pattern of isotopic variability in peatland water, and such site-scale variations can be further linked to water flow patterns. For example, Isokangas *et al.* (2017) used water isotope tracers to map hotspots of groundwater recharge into near-surface pore water and found this to be spatially heterogeneous within a peatland complex of about 4 km$^2$. Ronkanen & Kløve (2007, 2008) used water isotope tracers to detect ditch-affected preferential flow paths and evaporation-affected dead zones at a site scale of a few hundred metres, in peatlands treating municipal wastewater. In a small patterned peatland, Carrer *et al.* (2016) found that isotope ratios of pool water have increasing evaporative enrichment from upstream to downstream, indicating the cascading streamflow process and mixing between pools. Other studies have also found clear gradients of evaporative enrichment in water at the peatland surface within a site, such as from the margin to the central open expanse of a small peatland complex across a distance of about 100 m (Graham *et al.* 2016, Sprenger *et al.* 2017), or along the topography-driven flow direction in a large peatland complex over several kilometres (Gibson *et al.* 2022).

Despite the recognised importance and high diversity of hydrological processes in peatland ecosystems, the applications of water isotope tracers in studying peatland hydrology remain limited in number. Therefore, we cannot fully document different spatial patterns of isotopic variability in peatland water across various types of peatlands and different climates worldwide. However, the current development of laser spectroscopy techniques (Maselli *et al.* 2013) promises a potentially inexpensive and rapid approach for characterising the spatial heterogeneity of hydrological conditions and processes in peatlands including their water sources, turnover and flow patterns at whole-site scale. Additionally, no study has established an interpretative framework for spatial isotope data, nor linked spatial isotopic variations with quantitative models of isotopic fractionation. Thus, we do not yet fully understand how different factors affect or control spatial isotopic variations in peatland water. These gaps in data and knowledge present obstacles to the general use of water isotope tracer techniques to complement traditional field and laboratory methods for investigating peatland hydrology.

There have been decades of investigations of regional peatlands in Northeast China, which is the main region for peatlands in China. The best-known studies are those reconstructing long-term environmental changes and carbon accumulation histories (Hong *et al.* 2000, Schröder *et al.* 2007, Zhou *et al.* 2010, Xing *et al.* 2015, Dong *et al.* 2021). These peatlands are globally unique for being affected by the monsoon climate, with strong and synchronous seasonality in precipitation and temperature (Zhao *et al.* 2014). However, they are poorly represented in the current literature on modern peatland hydrology (Wei *et al.* 2022). In this study, we characterise and analyse the spatial pattern of isotopic variability in water at the surfaces of three peatlands in the Changbai Mountains, Northeast China, complementing existing literature on peatland isotope hydrology literature because this focuses heavily on European and North American peatlands at higher latitudes. We also develop a simple one-dimensional model of isotopic fractionation to gain a generalised understanding of how different factors control spatial isotopic variations in peatland water. Our study demonstrates that this spatial approach can differentiate surface hydrology among different hydrogenetic peatland types, with potential for quantitative inferences.

## METHODS

### Study sites and sampling

Our study sites are located in the Changbai Mountains, Jilin Province, Northeast China (Figure 1a). The region has a temperate continental monsoon climate with, depending on the elevation and aspect, a mean annual air temperature between -7 °C and 4 °C and mean annual precipitation between 700 mm and 1400 mm. It has strong temperature seasonality (Figure 1b). Over 80 % of precipitation is concentrated in the summer half-year (May–October; Figure 1b). The mean relative humidity is as high as about 80 % during June–September (Figure 1b). The region is peatland-rich due to cool and wet conditions, widespread volcanic terrain with local valleys and depressions, and the resultant poor drainage (Bao *et al.* 2010, Xu *et al.* 2024). This study investigates three peatland sites: Hani, Jinchuan, and Laolike (Figures 1c–e).

Hani peatland (42.22 °N, 126.52 °E, elevation 900 m a.s.l., area 16 km$^2$) is a sloping poor fen on the western flank of the Changbai Mountains, located within a valley formed by late Quaternary volcanic lava (Figures 2a,b). As a Ramsar wetland site (Site Number 2350), it is a mesotrophic (pH 4.5–5.5) headwater peatland with thick peat deposits that have a maximum depth of at least 9 m (Zhang *et al.* 1997, Zhou *et al.* 2010). The local elevation is higher in the north and south than in the centre and higher in the

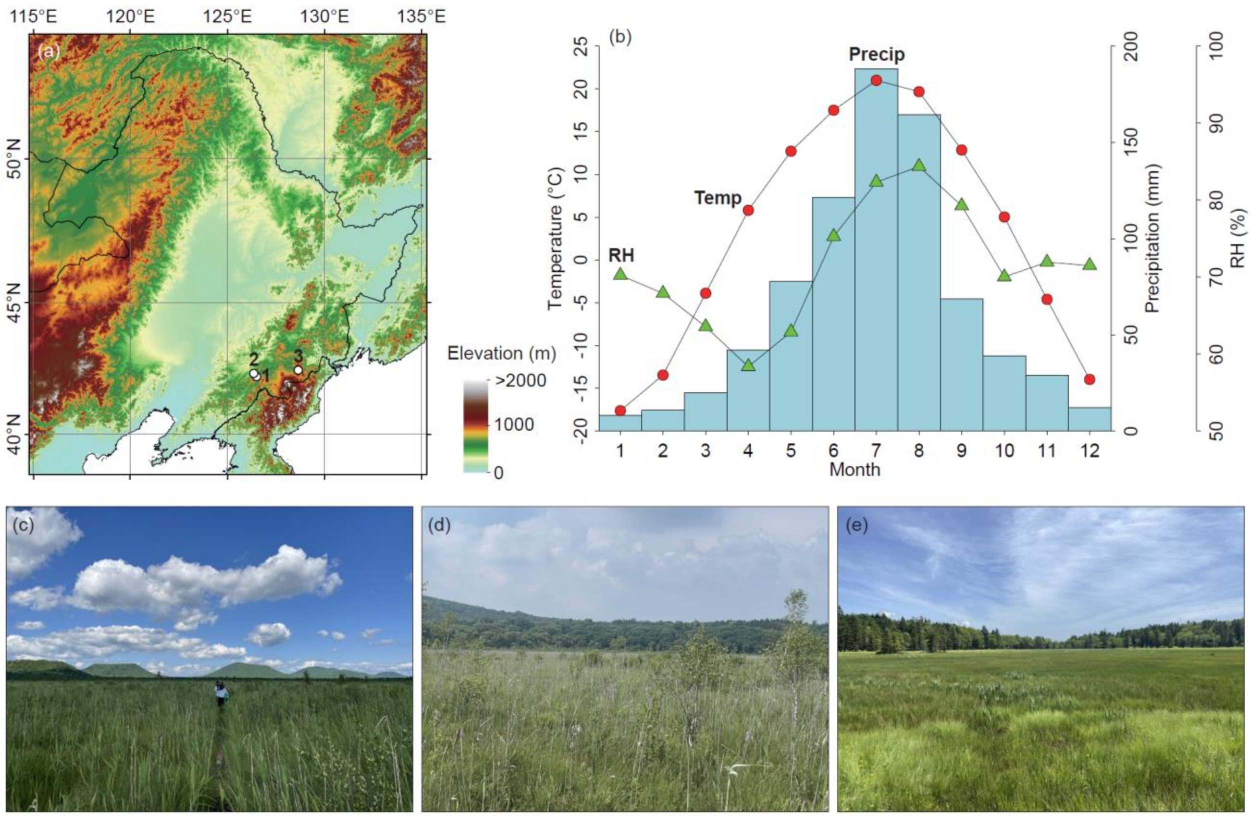


Figure 1. Context of the study region and field images of peatland sites. (a) Locations of study sites (1: Hani peatland; 2: Jinchuan peatland; 3: Laolike peatland) shown on a map of Northeast China coloured based on elevation. (b) Twelve-monthly means of air temperature (red dots), precipitation (columns) and relative humidity (RH; green triangles) from weather station data (1955–2024) from Jingyu County (30 km Northeast of Hani peatland), showing regional monsoon climate characteristics. (c) Field view of Hani peatland. (d) Field view of Jinchuan peatland. (e) Field view of Laolike peatland.

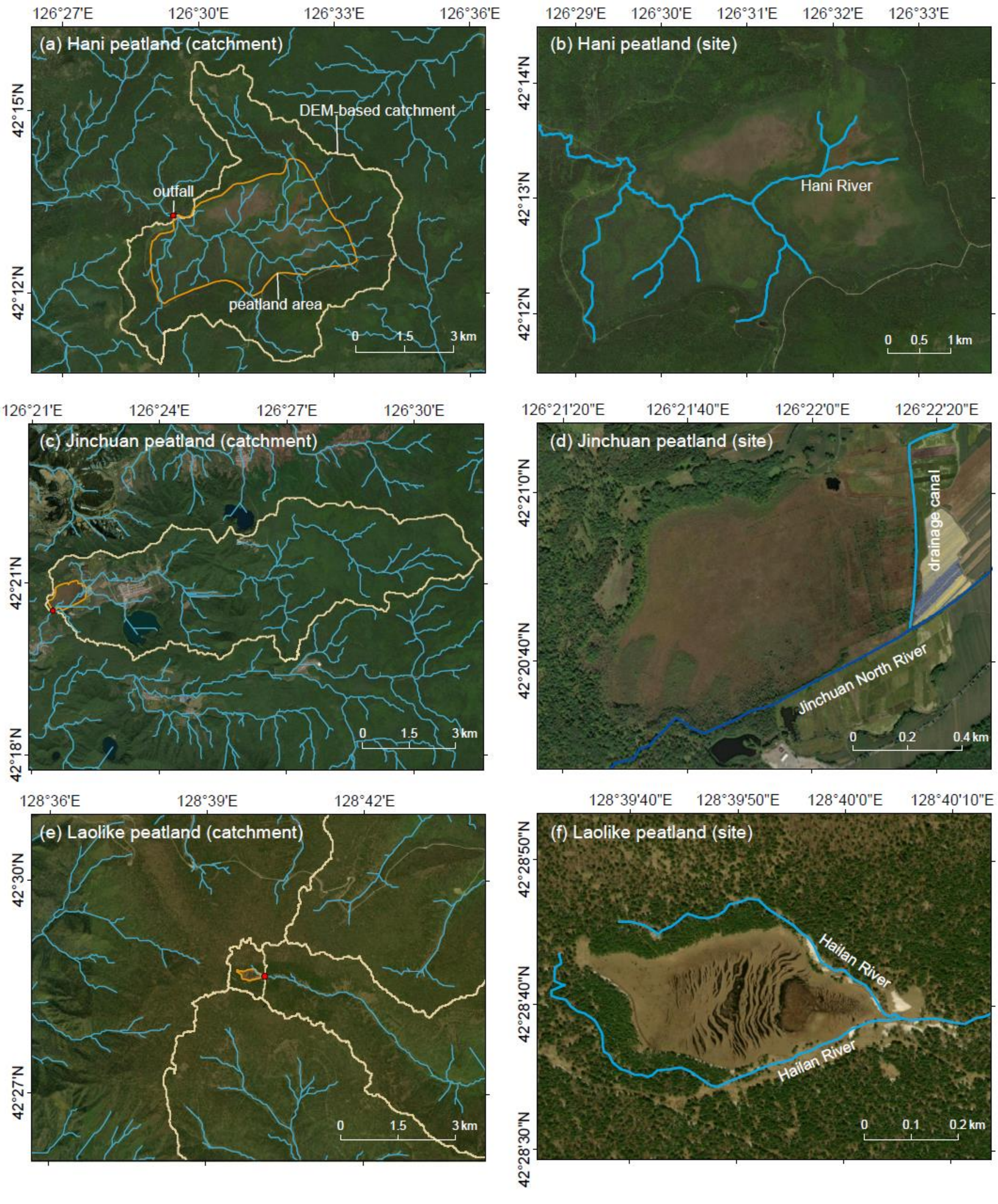


Figure 2. An overview of the peatland sites. (a) Hani peatland area (orange boundary) and its context within the upstream catchment area (yellow boundary). The upstream catchment area is determined based on flow direction and accumulation analysis of the digital elevation model (DEM; "SRTM 1 Arc-Second Global" available on the USGS EarthExplorer) and the outfall of the DEM-based flow network (blue lines) that drains through the peatland. (b) Hani peatland from satellite image with superposed course of Hani River (not the DEM-based flow network). (c) Similar to (a) but for Jinchuan peatland. (d) Jinchuan peatland from satellite image, with the drainage canal to the east and the straightened Jinchuan North River to the south superposed. (e) Laolike peatland and its context within the regional catchment system. (f) Laolike peatland from satellite image with superposed course of Hailan River.

east than in the west. The slope is about 1 % (10 m elevation over 1000 m distance) in the northern part (Schröder *et al.* 2007). Hani River originates here, cutting through the middle, flowing westward and separating the peatland into several parts (Figure 2b). The hydrology of this site was characterised by Schröder *et al.* (2007) who classified this peatland as a "percolation mire" commonly found in the temperate zone (Joosten & Clarke 2002). More accurately, this sloping poor fen is fed by both precipitation and shallow seepage from the surrounding forested hillslope, receiving abundant water which flows through the gently sloping, hydraulically conductive surface and drains into the Hani River (Zhang *et al.* 1997, Zhou *et al.* 2010). The northern and southeastern areas have large open fields (Figure 2b). From the open fields to the surrounding upland or Hani River, the vegetation shifts from sedges (*Carex* spp.) and reeds (*Phragmites australis*) with peat mosses (*Sphagnum* spp.) to mixed larch trees (*Larix olgensis*) and shrubs (*Betula ovalifolia*, *Ledum palustre*, *Vaccinium uliginosum*), and finally to larch forest (Schröder *et al.* 2007).

Jinchuan peatland (42.35 °N, 126.36 °E, elevation 620 m a.s.l., area 0.76 $km^2$) is about 20 km away from Hani peatland but is much smaller in extent (Figures 2c,d). It is a eutrophic-mesotrophic (pH 5.6–6.0) peatland developed from a dammed lake on the river terrace, with a maximum peat depth of at least 6 m (Zhang *et al.* 1997, Zhang *et al.* 2019). The local elevation decreases very slightly from north to south, with a slope of about 0.2 % (1.2 m elevation over 600 m distance, estimated from a field-based high-resolution topographic elevation survey; Ma 2020). An early survey suggested that this horizontal poor fen is more affected by groundwater inflows compared to the Hani peatland (Zhang *et al.* 1997). Peatland vegetation is dominated by sedges, reeds and shrubs, as found in the Hani peatland, but peat mosses (mostly the fen species *S. palustre*) are less abundant. Since the 1950s the site has been affected by agricultural activities, with a drainage canal to the east and a straightened river (Jinchuan North River) to the south (Figure 2d), which has resulted in the loss of about 30 % of the original area and reduced the surface water inflow available to the current peatland. The area has been protected since 2003, but human-made landscape features are visible on the eastern side from satellite images (Figure 2d).

Laolike peatland (42.48 °N, 128.66 °E, elevation 1480 m a.s.l., area 0.13 $km^2$) is located at the top of Mt. Zengfengling (Figure 2e and f). It is a small west-east-oriented headwater peatland within a broad and shallow depression surrounded by forests and has a maximum peat depth of at least 7 m (Dong *et al.* 2021). The local elevation decreases from west to east, with a slope of about 2 % (10 m elevation over 500 m distance). This mountain-top site shows features of a sloping bog relying on precipitation as the source water. The northern, eastern and southern sides of the Laolike peatland are bounded by deep eastward-flowing headwater streams (Hailan River), which largely separate the site from catchment runoff (Figure 2f). The western area is relatively dry with abundant peat mosses (mostly bog species *S. fuscum*) that form large hummocks as a sign of ombrotrophy. Towards the east, there are north-south elongated pools of various sizes visible from satellite images (Figure 2f), but their boundaries were not immediately clear at the time of sampling in summer due to floating mat coverage and abundant standing water at the peatland surface. There, the vegetation is dominated by sedges with other monocots (e.g., *Eriophorum latifolium*).

We collected samples of water at the peatland surface in different locations at these sites during different campaigns. For Hani peatland, we collected 18 samples along a north–south transect in the northern area in July 2022 and 72 samples more extensively from both the northern and southeastern areas in August 2022. For Jinchuan peatland we collected 27 samples in October 2022 and 34 samples in June 2023, in a mesh-like network with approximately 100 m spacing between nodes. For Laolike peatland we collected 19 samples in July 2023 along two west–east transects. We also collected relevant river water samples during each campaign. Water samples were stored in HDPE bottles and filtered through a 1-μm cellulose acetate membrane before isotope analyses. Hydrogen ($\delta^2H$) and oxygen ($\delta^{18}O$) isotopic compositions were measured with the Picarro L2130-i at Northeast Normal University, and results were reported in δ-notation by convention. The analytical precision (1σ) is about 0.09 ‰ for $\delta^2H$ and 0.02 ‰ for $\delta^{18}O$, and accuracy is assured by calibration against three laboratory standards.

**Mechanistic modelling**

An idealised, one-dimensional mechanistic model is introduced here to simulate spatial isotopic variations in peatland water as it flows downslope through a horizontal transect of a hydraulically conductive surface peat layer and evaporates along the route under steady-state conditions, while neglecting water flows within the deep peat body. The formulation of this model is the same as that used to simulate spatial isotopic variations in atmospheric water vapour along a storm track. In that model, atmospheric water vapour advects over a transect and alters its balance through precipitation (efflux) and evapotranspiration (influx) (Chamberlain *et al.* 2014, Winnick *et al.* 2014). In this model, peatland water flows along a horizontal transect and undergoes changes in mass and isotopic balance due to evapotranspiration (efflux) and upward groundwater recharge (influx). The following differential equation can be derived, analogous to Equation 4 presented in Chamberlain *et al.* (2014):

$$-v\frac{d\delta_S}{dx}+\frac{G}{S}(\delta_G-\delta_S)-\frac{ET}{S}(\delta_{ET}-\delta_S)=0 \quad [1]$$

where $S$ is the thickness of the water flow, $ET$ is the evapotranspiration flux, $G$ is the groundwater flux, $\delta_S$, $\delta_G$, and $\delta_{ET}$ represent the isotopic compositions of peatland water (at the surface), groundwater influx and evapotranspiration efflux, respectively, $v$ is the horizontal flow velocity, and $x$ is the horizontal distance. The term $v$ can be expressed using Darcy's law as:

$$v=K_s\frac{\Delta H}{\Delta L} \quad [2]$$

where $K_s$ is the saturated hydraulic conductivity,and $\Delta H/\Delta L$ is the hydraulic gradient, i.e., the change in hydraulic head per unit distance.

For simplicity, we have made several assumptions to allow a generalised understanding of first-order model behaviours. First, we assume that the hydraulic gradient $\Delta H/\Delta L$ can be replaced by the topographic gradient, based on field observations indicating that the water table remains close to the peatland surface at all sites. Secondly, we assume that $G = ET$, meaning that the evapotranspiration efflux from water at the peatland surface would be quickly replenished by an equivalent upward influx of groundwater recharge from the deep peat body. Under this assumption, the thickness of the water flow remains unchanged across the transect, simplifying Equation 1 to:

$$\frac{d\delta_S}{dx}=\frac{ET}{S}\left(K\frac{\Delta H}{\Delta L}\right)^{-1}(\delta_G-\delta_{ET}) \quad [3]$$

However, these two assumptions may be invalid for sites having substantial spatiotemporal variability in water table. Thirdly, we assume that $\delta_G$ is homogeneous across the transect and that $\delta_G = \delta_S(x{=}0)$. This means that the deep groundwater has the same isotopic composition as the inflow initiating the model. This assumption can be relaxed if site-specific $\delta_G$ and $\delta_S(x{=}0)$ data are available.

The model neglects precipitation influx because it would be functionally similar to the groundwater recharge term that has been assumed to replenish the thickness of the water flow. In other words, the groundwater recharge term has implicitly incorporated the effect of precipitation influx to maintain the water balance of the peatland catchment. This approach may not always be appropriate, and Equation 1 should be modified to incorporate an independent precipitation term if the isotopic composition of precipitation differs strongly from $\delta_G$.

To explore model behaviours, we create a control simulation using suitable model variables chosen to match the pattern of field data collected at Hani peatland in July 2022, where and when a clear spatial $\delta^{18}O$ gradient was found in water at the peatland surface (see the following section). Among model variables, $ET$ is estimated based on its linear relationship (with a slope of about 0.6) with potential evapotranspiration (determined from the Thornthwaite method) established for fen peatlands (Wu *et al.* 2010, Runkle *et al.* 2014). Schröder *et al.* (2007) measured multiple vertical profiles of $K_s$ at Hani peatland. Their mean values decrease from $8\times10^{-3}$ m s$^{-1}$ at 5 cm depth to $10^{-3}$ m s$^{-1}$ at 35 cm depth and become as low as $10^{-5}$ m s$^{-1}$ at 100 cm depth. Note that anisotropy was not considered in previous $K_s$ measurements, and horizontal $K_s$ should be more appropriate as input for the model (Morris *et al.* 2019, Wang *et al.* 2021). We set $K_s$ at a high value of $10^{-2}$ m s$^{-1}$, close to the interpolated $K_s$ value at the surface. We set $S$ at 24 cm, estimated by multiplying wet bulk density (0.9 g cm$^{-3}$), peat water content (90 %), and depth of the low-$K_s$ layer (30 cm). This implementation considers that peatland water stored in the top 30 cm peat layer is well mixed but preferentially flows through the uppermost surface peat layer, given the ubiquitous standing water at this site (Holden 2005). The term $\delta_{ET}$ is calculated at each numerical step based on a flexible parameterisation developed by Xia & Winnick (2021) (their Equation 10), which requires several additional inputs including temperature (18 °C), relative humidity (85 %), aerodynamic exponent (0.5, i.e., the "wet soil" value; Mathieu & Bariac 1996) and transpiration fraction (75 %; Admiral & Lafleur 2007). The meteorological data (July 2022) are based on the weather station record from Jingyu County (Figure 1b), 30 km northeast of Hani peatland. These model variables are all set as constants across the transect for simplicity, but they can be set as an array of values to capture locally changing conditions such as possibly lower $K_s$ in the downslope marginal peat (Baird *et al.* 2008). On the basis of the control run, we vary key variables for a sensitivity analysis to demonstrate how different variables affect the model outputs, and discuss the implications for other sites.

The source code for running the model is available from the GitHub repository (https://github.com/zhx215/peatland-surface-water-isotope-model). A schematic diagram of the model structure is shown in Figure 7a, later in this article.

## RESULTS

### Isotopic measurements of peatland water and river water

At Hani peatland, the $\delta^2$H and $\delta^{18}$O values of the 18 peatland water samples collected in July 2022 from the northern area range from -83.9 ‰ to -72.6 ‰ and from -12.0 ‰ to -10.5 ‰, respectively (Figures 3 and 6a). These data clearly show a spatially increasing trend from north to south along the topographic downslope direction towards the river, with a regression coefficient of 6.5 (Figures 3 and 6b). The low regression coefficient (< 8) indicates the role of evaporation (Gat 1996), and the regression line can be seen as the isotopic local evaporation line (LEL). The $\delta^2$H and $\delta^{18}$O values of the 72 water samples collected in August 2022 vary within narrower ranges, from -79.3 ‰ to -73.7 ‰ and from -11.4 ‰ to -10.5 ‰, respectively, even though sampling was more extensive, aiming to cover both northern and southeastern areas (Figures 3 and 6b). These data also show a spatially increasing trend along the topographic downslope direction, specifically from north to south in the northern area and from east to west in the southeastern area (Figure 3), and together yield an LEL slope of 6.9 (Figure 6b). The $\delta^2$H and $\delta^{18}$O values for river water samples in each sampling campaign are within the respective ranges of variability in peatland water (Figure 6b).

At Jinchuan peatland, the $\delta^2$H and $\delta^{18}$O values of the 27 peatland water samples collected in October 2022 range from -72.3 ‰ to -66.3 ‰ and from -10.5 ‰ to -9.6 ‰, respectively, except for an anomalous sample collected from the human-made agricultural pond in the northeast corner with a $\delta^2$H value of -65.4 ‰ and a $\delta^{18}$O value of -8.5 ‰ (Figures 4a and 6c). That anomaly stands out on the $\delta^2$H-$\delta^{18}$O biplot, being plotted at the upper right side of the rest of the data (Figure 6c). Omitting the anomaly, the data yield an LEL slope of 6.6 (Figure 6c). The $\delta^2$H and $\delta^{18}$O values of the 34 water samples collected in June 2023 are clustered in the range -66.8 ‰ to -59.3 ‰ and from -10.0 ‰ to -8.9 ‰, respectively, except for four high (less negative) anomalies (Figure 6c). These four anomalies have $\delta^2$H and $\delta^{18}$O

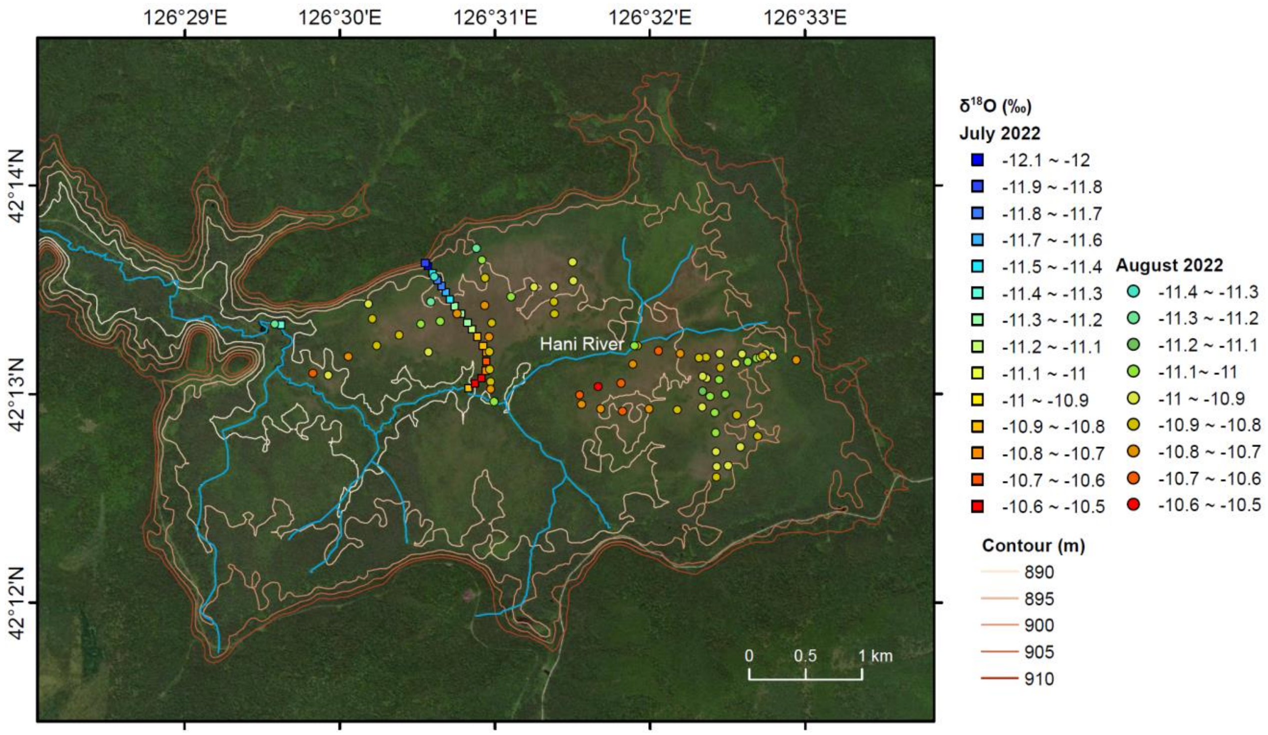


Figure 3. Spatial map of measured $\delta^{18}$O values (coloured symbols) in water at the peatland surface at Hani peatland. Square and circle symbols represent data collected during sampling campaigns in July 2022 and August 2022, respectively. The Hani River and selective reference elevation contours (based on the same "SRTM 1 Arc-Second Global") are also shown to provide the topographical context for this site.

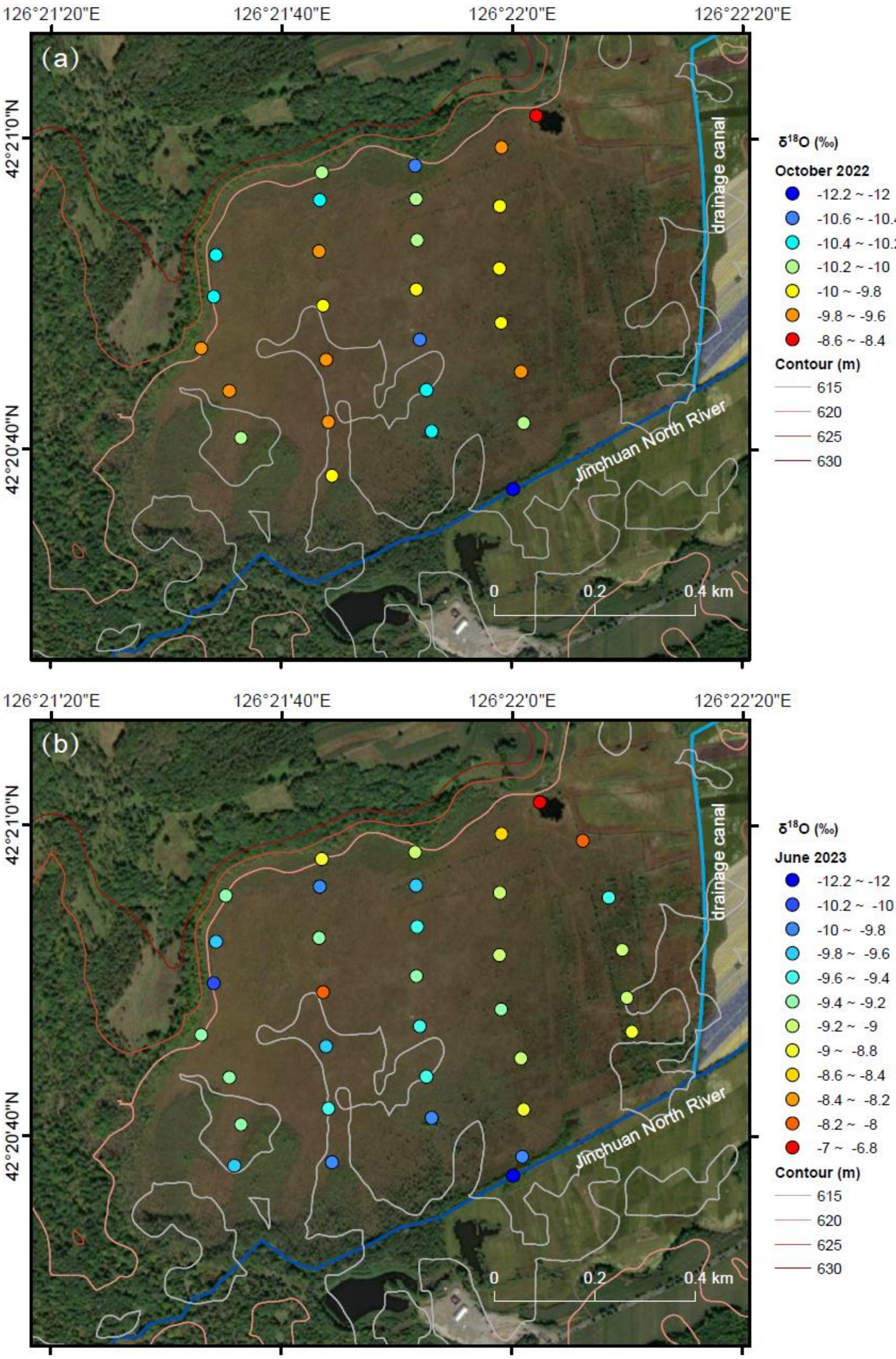


Figure 4. Spatial maps of measured $\delta^{18}O$ values (coloured symbols) in water at the peatland surface at Jinchuan peatland from two sampling campaigns in (a) October 2022 and (b) June 2023. The drainage canal to the east and the straightened Jinchuan North River to the south are also shown along with selected elevation contours, similar to Figure 3. Note that the colour scale values are not all consecutive, and differ between the two subplots.

values ranging from -59.1 ‰ to -56.0 ‰ and from -8.5 ‰ to -6.9 ‰, respectively (Figure 6c). One of them was collected at the centre of the peatland and the other three from the agricultural pond or its vicinity (Figure 4b). These anomalies also stand out on the $\delta^2H$-$\delta^{18}O$ biplot by plotting at the upper right side of the rest of the data, while the latter yield an LEL slope of 6.2 (Figure 6c). Additionally, for both sampling campaigns, there is an emerging spatial pattern in the peatland water $\delta^{18}O$ values in that they are slightly lower close to the northern, northwestern and southern sides of the peatland (Figure 4). The $\delta^2H$ and $\delta^{18}O$ values for river water samples are about -85 ‰ and -12 ‰, respectively, i.e. much lower than those for peatland water (Figure 6c).

At Laolike peatland, the $\delta^2H$ and $\delta^{18}O$ values of the 19 peatland water samples collected in July 2023 range from -78.9 ‰ to -66.2 ‰ and from -11.2 ‰ to -8.8 ‰, respectively (Figure 6d). The $\delta^{18}O$ data for peatland water are spatially heterogeneous (Figure 5). These data form an LEL slope of only 4.4 on the $\delta^2H$-$\delta^{18}O$ biplot (Figure 6d). The $\delta^2H$ and $\delta^{18}O$ values for river water samples are about -96.5 ‰ and -14 ‰, i.e. much lower than for peatland water (Figure 6d) and showing similarity to Jinchuan peatland.

**Model simulations of horizontal isotopic variations in peatland water**

The control simulation successfully reproduces the continuously increasing trend in peatland water $\delta^{18}O$ towards the downslope direction, as well as the LEL slope (simulated value: 6.4; measured value: 6.5) between $\delta^2H$ and $\delta^{18}O$ in our field data collected in the northern open field of Hani peatland in July 2022 (Figures 3 and 7b). The $R^2$ value is 0.92 and the root mean square error (RMSE) is 0.13 ‰ without additional parameter fitting.

In the sensitivity analysis (Figure 7b), an order-of-magnitude difference in hydraulic conductivity $K_s$ strongly affects the simulation output. Specifically, a higher $K_s$ results in a much shallower increasing trend in peatland water $\delta^{18}O$ across the transect, whereas a lower $K_s$ results in a steep increase in the first 200 m of the transect followed by a plateau in peatland water $\delta^{18}O$. This plateau behaviour indicates that the isotopic composition of the evapotranspiration efflux is balanced by the groundwater influx replenishing the peatland water. The same simulation outputs can be derived by varying the relative evapotranspiration rate $ET/S$ in the opposite direction or the hydraulic gradient $\Delta H/\Delta L$ in the same direction as $K_s$. As

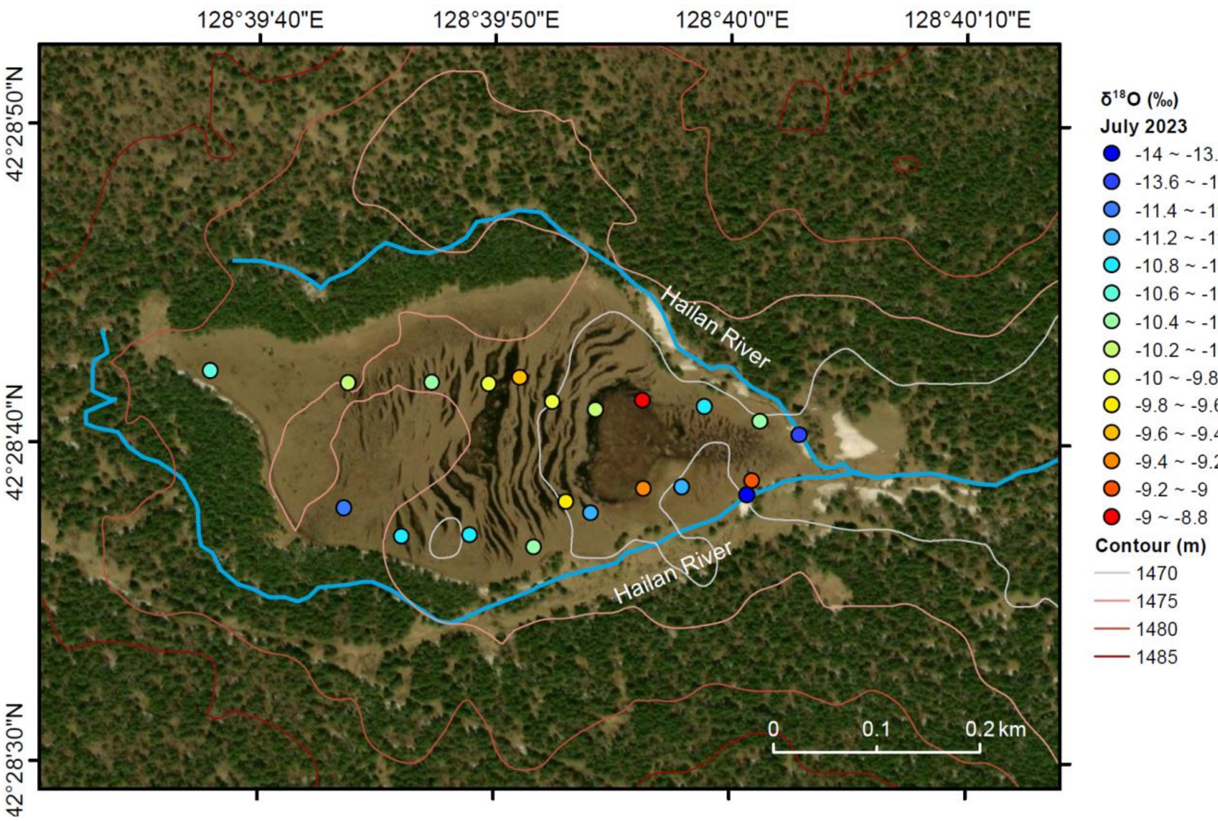


Figure 5. Spatial map of measured $\delta^{18}O$ values (coloured symbols) in water at the peatland surface at Laolike peatland. Hailan River and selective elevation contours are also shown, similar to Figure 3. Note that the colour values are not all consecutive.

directly explained in Equation 3, this is because a higher $K_s$ increases the flow velocity, reduces the travel time, and reduces the total flux of evapotranspiration - a consequence that can also be produced by lower $ET/S$ or higher $\Delta H/\Delta L$ alone. Because transpiration does not fractionate water isotopes but evaporation enriches heavy isotope species in liquid water, a higher transpiration fraction $T/ET$ results in a much shallower increasing trend in peatland water $\delta^{18}O$ across the transect, similar to the effect of higher $K_s$. Conversely, a lower $T/ET$ results in a steeper increasing trend in peatland water $\delta^{18}O$ across the entire transect without showing the plateau behaviour. Finally, relative humidity slightly affects the spatial gradient of peatland water $\delta^{18}O$, but it is the only factor that controls the slope of the LEL, with lower relative humidity associated with a lower LEL slope (Figure 7c).

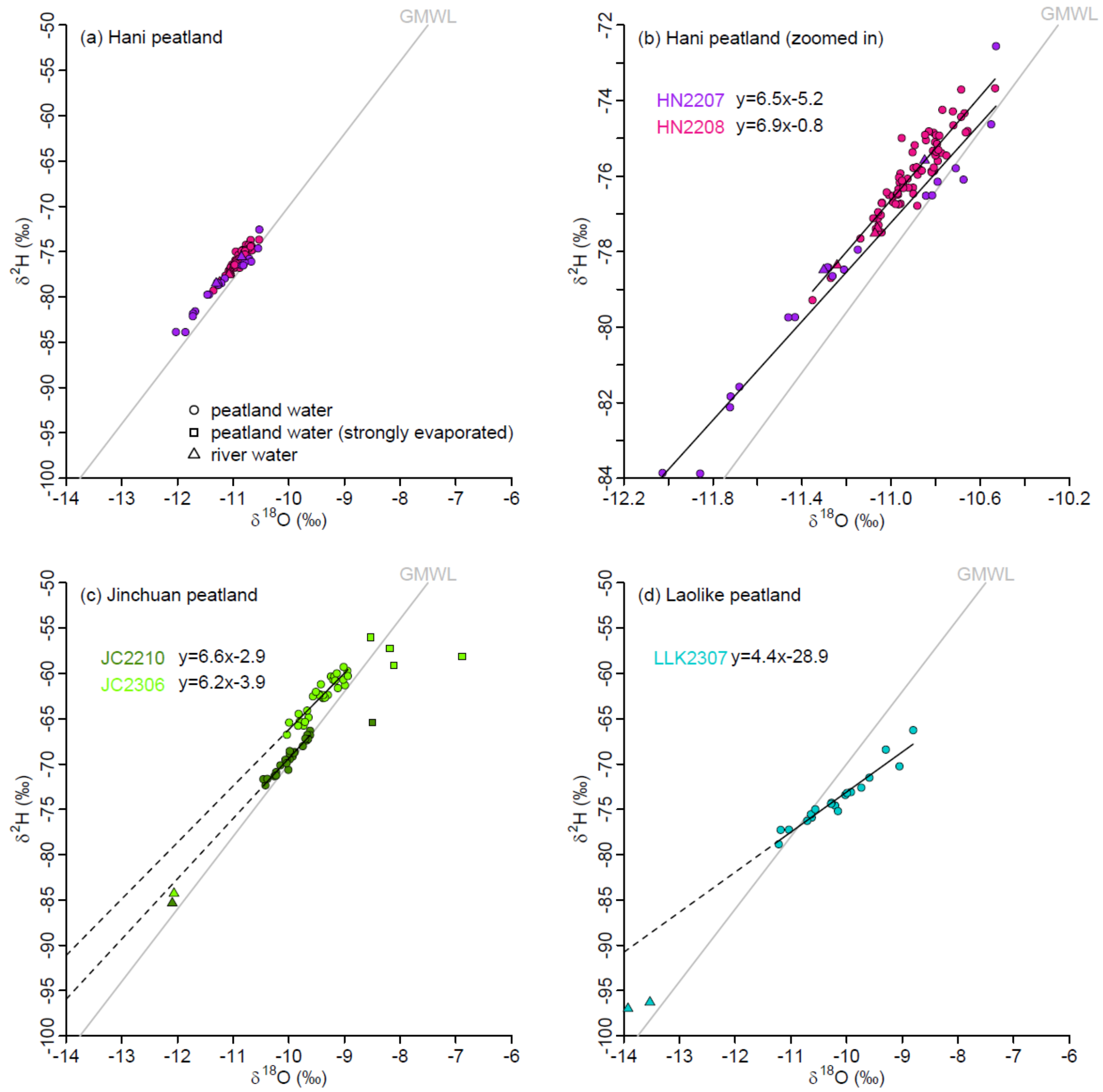


Figure 6. Biplot between $\delta^2H$ and $\delta^{18}O$ for peatland water and river water samples at the different sites. (a) Hani peatland. (b) Hani peatland, the same as (a) but with coordinate axes adjusted to narrower ranges. (c) Jinchuan peatland. (d) Laolike peatland. Data from different campaigns are distinguished by colour (HN2207 means samples collected in July 2022 from Hani peatland, and likewise for others; JC = Jinchuan peatland, LLK = Laolike peatland). Regression lines and equations indicating local evaporation lines (solid black lines) derived from these data (after excluding samples with distinct evaporative enrichment) are also plotted. For Jinchuan and Laolike peatlands, these lines are extended to lower δ-values (dashed black lines). The grey line in each subplot is the Global Meteoric Water Line ($\delta^2H = 8\times\delta^{18}O + 10$).

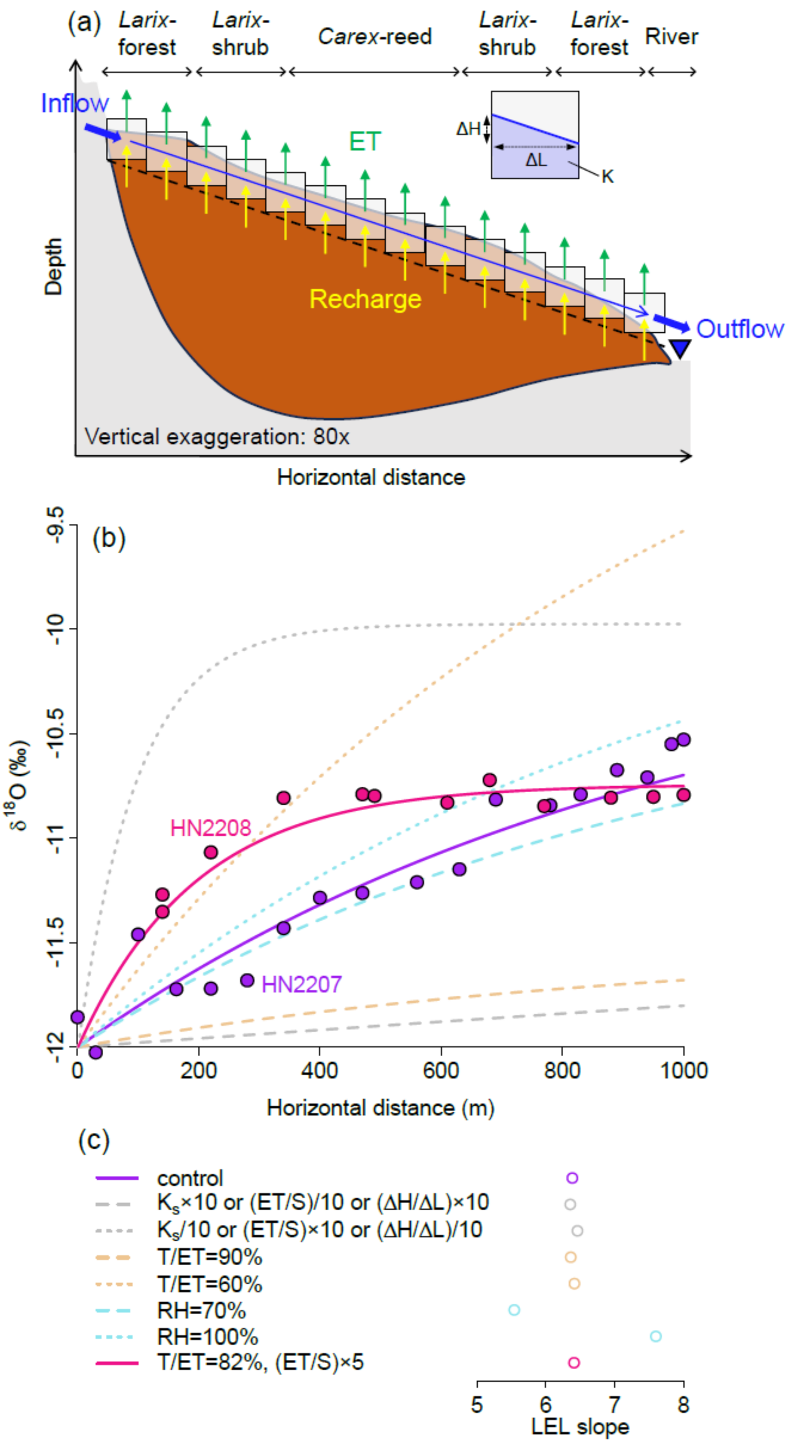


Figure 7. Model simulations of horizontal isotopic variations in peatland water, using Hani peatland as the modelling target. (a) Schematic diagram of one-dimensional model as well as the cross-section and vegetation zonation along the north–south transect in the northern open field of Hani peatland, modified from Schröder *et al.* (2007). (b) Simulated peatland water $\delta^{18}O$ variations against horizontal distance assuming peatland water is flowing downslope within a one-dimensional transect. The control run aims to reproduce the field sample data collected from the north–south transect in the northern open field of Hani peatland in July 2022. Other simulations are created to show the sensitivity of results to key model variables. Field sample data from August 2022 and the simulation tuned to match these data (by changing $T/ET$ to 82 % and multiplying $ET/S$ by 5) are also plotted. These data are projected to the same 1-km transect. The lower panel beside the legend shows the slope of the local evaporation line in each model run, regressed through the model output of $\delta^{2}H$ and $\delta^{18}O$.

## DISCUSSION

Isotope ratios of water at the peatland surface, surveyed at three sites within the same region, reveal an intriguing diversity of spatial patterns. These new data offer an opportunity to gain insights into the spatial heterogeneity of hydrological conditions and processes specific to each site. The mechanistic model we developed aims to mathematically represent the key factors and processes controlling spatial isotopic variations and support data interpretations. Although this model is simple and highly idealised, it provides a theoretical basis for generating a flexible interpretive framework and is a first step toward making quantitative inferences about peatland hydrology using water isotope data in the future. Specifically, the model predicts the expected spatial patterns of isotopic variability in water at the surfaces of peatlands dominated by horizontal surface flows. The importance of horizontal surface flows in peatland hydrology has been shown in multiple studies using water isotope tracers (Ronkanen & Kløve 2007, Rydin & Jeglum 2013, Carrer *et al.* 2016, Sprenger *et al.* 2017, Gibson *et al.* 2022). If the field data match these expected patterns, we can infer that horizontal surface flows are dominant and it is likely that data-constrained model simulations can be used to infer poorly known factors such as the relative evapotranspiration rate *ET*/*S* and transpiration fraction *T*/*ET*. If not, we may acknowledge that simple horizontal surface flow patterns are not strictly attained in the studied peatlands, prompting us to investigate potential reasons based on insights gained from model simulations. The addition of river water isotope data can further constrain models of peatland hydrology in a catchment context.

In the subsections below, we use our three sites belonging to different hydrogenetic types as examples, along with other sites described in the literature, to demonstrate that the spatial isotopic variations in peatland water can distinguish site-scale characteristics of water sources, turnover and flow patterns (Figure 8), and can be interpreted quantitatively.

### Hani peatland

Hani peatland is the largest site examined in this study but it has the smallest range of peatland water $\delta^{18}O$ variability, at 1.5 ‰ and 0.9 ‰, respectively, for two sampling campaigns (Figure 6a). Nevertheless, these $\delta^{18}O$ data exhibit clear spatial patterns, with the most notable feature being the increasing trend from north to south in the northern area in both sampling campaigns (Figure 3).

The control run of the mechanistic model successfully reproduces the gradually increasing trend in peatland water $\delta^{18}O$ and the LEL slope

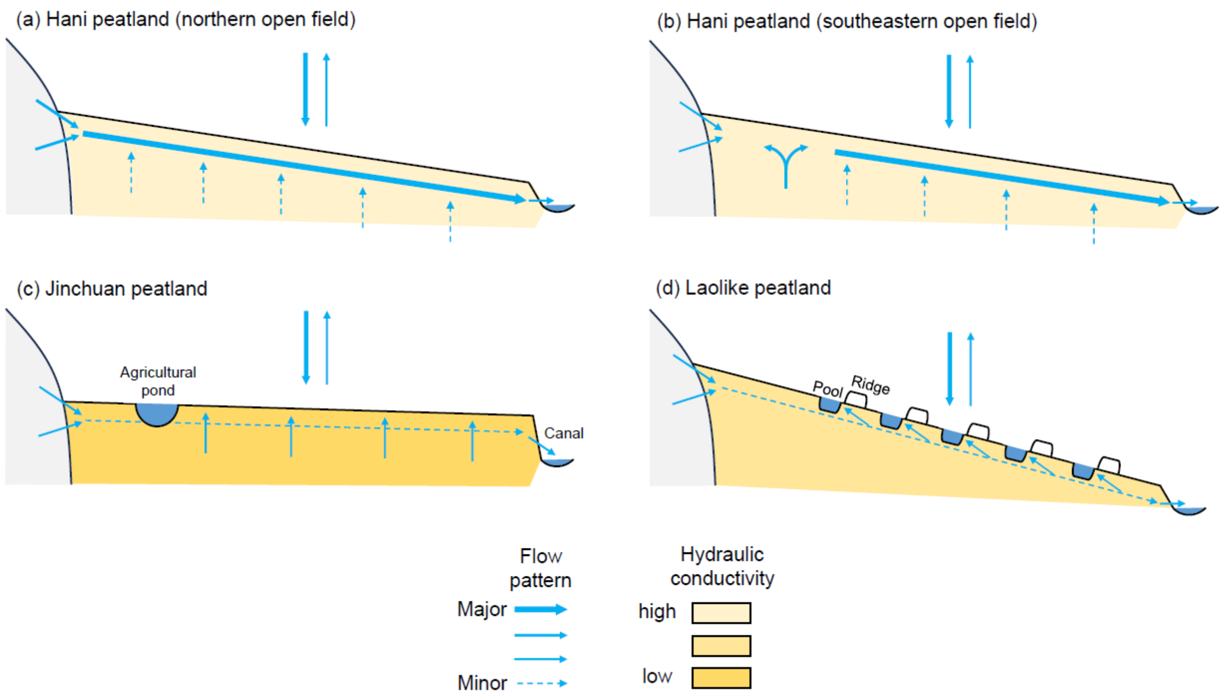


Figure 8. Conceptual diagrams for inferred flow patterns at the three peatlands based on the analysis of water isotope data. (a) The northern open field of Hani peatland. (b) The southeastern open field of Hani peatland. (c) Jinchuan peatland. (d) Laolike peatland.

observed during the July 2022 campaign (Figure 7b). As supported by the LEL-related low regression coefficient (< 8) between $\delta^2$H and $\delta^{18}$O (Figure 6b), this spatial pattern results from progressive evaporation-induced isotopic enrichment as water at the peatland surface moves slowly downslope (Sprenger *et al.* 2017, Gibson *et al.* 2022). The enrichment reaches its maximum before the water drains into the Hani River. However, peatland water $\delta^{18}$O data from a similar north–south transect (not exactly the same sampling locations), collected in the August 2022 campaign, show a plateau behaviour over the second half of the transect (Figure 7b). Our model sensitivity analysis suggests that this plateau behaviour may occur under low hydraulic conductivity $K_s$, high relative evapotranspiration rate $ET/S$, or low hydraulic gradient $\Delta H/\Delta L$ (Figure 7b). Although our model demonstrates capacity to represent the plateau behaviour observed in our data, the reason for the change in the spatial pattern of isotopic variability over the course of a single month under similar field conditions remains unclear. Given that $K_s$ and $\Delta H/\Delta L$ should be stable, reproducing the trend in peatland water $\delta^{18}$O data collected in the August 2022 campaign requires a fivefold increase in $ET/S$ and a slight increase in the transpiration fraction $T/ET$ to 82 % ($R^2$ = 0.90, RMSE = 0.07 ‰) (Figure 7b). This inference remains to be validated but highlights the important limitations of our simplified model.

In the southeastern area, there is another increasing trend in peatland water $\delta^{18}$O from east to west along the downslope direction. However, the lowest $\delta^{18}$O values appear to be located in the central-east area rather than at the peatland margin, which would be expected to receive the newest, unevaporated seepage from the adjacent forested hillslope (Figure 3). This feature may result from locally different source water with a slightly higher $\delta^{18}$O signal or from groundwater upwelling in the central-east area and reversing the flow direction toward the margin (Devito *et al.* 1997, Hokanson *et al.* 2020).

Overall, our peatland water isotope data suggest that the surface water reservoir at this site, which has strong vegetation zonation (Figure 7a), is largely well-connected and dominated by pervasive surface flow driven by the large-scale topographic gradient, despite a possible hint of local flow reversal that warrants further investigation (Figures 8a,b). Isotope data for water from the Hani River, which is indistinguishable from peatland water on the $\delta^2$H-$\delta^{18}$O biplot (Figure 6b), further suggest that, in a catchment context, this large headwater peatland occupying about 40 % of the upstream catchment area is indeed the major transit zone for catchment water being routed to the river with high connectivity (Figure 2a). Overall, the inferred peatland hydrology, based on spatial isotope data, is consistent with the seminal work of Schröder *et al.* (2007), who suggested that this site is a pristine sloping "percolation mire" in the temperate zone, characterised by low degree of peat decomposition, high surface hydraulic conductivity, and persistently wet conditions.

**Jingchuan peatland**

Jinchuan peatland does not show the same spatial pattern of isotopic variability as found in Hani peatland. Using the distributed hydrological model MIKE SHE with a field-based high-resolution topographic elevation survey, a previous study suggested that the site should receive surface inflow from the northern and western margins (due to surface topography) and that water at the peatland surface should flow from north to south, draining into the Jinchuan North River following the topographic downslope gradient (Ma *et al.* 2016, Ma 2020). Although there are signs of unevaporated seepage in the northern and northwestern corners, there is no increasing trend in peatland water $\delta^{18}$O from north to south as would be expected from a process of progressive evaporation-induced isotopic enrichment (Figures 4 and 6c). Rather, $\delta^{18}$O values appear to be slightly lower near the southern side of the peatland (in particular during the June 2023 campaign) and spatially heterogeneous over other parts of the peatland (Figure 4).

A notable feature is the occurrence of distinct isotopic anomalies, some associated with the human-made agricultural pond in the northeast corner and one found in the central open field of the peatland, specifically from the June 2023 campaign (Figure 4). This central location has fewer shrubs and trees and is most exposed to solar heating and evaporation (Graham *et al.* 2016). These isotopic anomalies, falling way off from the LEL formed by the other data on the $\delta^2$H-$\delta^{18}$O biplot (Figure 6c), clearly indicate their distinct evaporative enrichment histories. In fact, such isotopic anomalies, plotting in the lower right space of the Global Meteoric Water Line, are commonly found in lakes with high evaporation : inflow ratios and long residence times (Gat 1996, Gibson *et al.* 2016, Vystavna *et al.* 2021).

Together, the absence of model-predicted progressive evaporation-induced isotopic enrichment downslope and the occurrence of local lake-like isotopic signatures within a peatland (especially in the central open field) are two strong indicators of poor surface hydrological connectivity preventing the dominance of horizontal flows (Isokangas *et al.* 2017). It is likely that this finding is primarily related to the gentle slope (about 0.2 %) of the horizontal poor fen and low hydraulic conductivity of the peat (about $10^{-5}$ m/s at 20 cm and between $3\times10^{-6}$ m/s and $5\times10^{-6}$ m/s at greater depths, based on measurements from 40 profiles; Tan 2012). These values are about two orders of magnitude lower than in Hani peatland due to human-enhanced drainage, which has lowered the water table and increased peat decomposition (Holden *et al.* 2006, Hribljan *et al.* 2014, Young *et al.* 2017, Chen *et al.* 2024). Measurements from previous studies show a layer of unusually high dry bulk density (about 0.2 g $cm^{-3}$) near the peatland surface (Bao *et al.* 2010, Sun *et al.* 2019), potentially due to drainage-enhanced decomposition (Liu *et al.* 2020). Both topographic and hydraulic factors would reduce flow velocity and increase the local residence time of peatland water (Figure 8c). The spatially heterogeneous variations of peatland water $\delta^{18}O$ also reflect more complex source water characteristics at this site arising from vertical flows, with a previous study suggesting possible groundwater influence (Zhang *et al.* 1997; Figure 8c).

Isotope data for Jinchuan North River water are distinctly lower than for peatland water and do not fall on the extrapolated LEL (Figure 6c). However, this isotopic disconnection is not surprising given the size and context of the site within the catchment. Specifically, the isotopic signature of river water collected beside the peatland integrates all upstream catchment runoff over a forested area of 43 $km^2$, whereas Jinchuan peatland has a more local water source and occupies only about 2 % of the upstream catchment area (Figure 2c).

**Laolike peatland**

Progressive evaporation-induced isotopic enrichment towards the downslope direction is also not observed at Laolike Peatland. The evaporation-driven peatland water $\delta^{18}O$ variability is spatially heterogenous and has a wider range than at other sites (Figure 6d), again indicating that the site has poor surface hydrological connectivity. This finding can be attributed to both the hydraulic structure of the peat and the water balance condition of the peatland.

First, Laolike peatland has many elongated pools oriented perpendicular to the slope direction (Figure 5). This surface patterning is a pronounced landscape feature characterising many peatlands (Rydin & Jeglum 2013). Previous studies suggest that pool formation mainly involves the effect and feedback of locally lower hydraulic conductivity, which can facilitate water accumulation and ponding upslope of linear ridges (Swanson & Grigal 1988, Couwenberg & Joosten 2005, Eppinga *et al.* 2009). Therefore, the patterning of peatland pools should not only increase the residence time of peatland water by buffering the water flow (Li *et al.* 2024) but also enhance the heterogeneity in peatland water residence time by segmenting individual pools. The hydraulic conductivity of peat at this site (about $10^{-4}$ m/s at 20 cm and $3\times10^{-5}$ m/s at 80 cm, based on measurements from four profiles in non-pool areas; Li *et al.* 2025) is intermediate - higher than that of drainage-affected Jinchuan peatland but still lower than that of the natural “percolation” Hani peatland. These factors together enhance the extent and heterogeneity of evaporative enrichment signatures, even though the site has developed on a steep slope (2°) that would otherwise favour rapid flows (Figures 5 and 8d).

Secondly, Laolike peatland is a rain-fed peatland in a headwater catchment (Figure 2e), with water balance dominated by precipitation and evapotranspiration fluxes. Its western side is likely to be the only area allowing direct surface inflow into the peatland, whereas its northern and southern sides closely neighbour two downcutting streams that shortcut the hillslope runoff (Figure 5). The low throughput from catchment runoff would further increase the residence time of peatland water.

These two factors are supported by the low LEL slope between $\delta^2H$ and $\delta^{18}O$ in peatland water collected in July 2023 (Figure 6d), which cannot be explained by the high relative humidity in summer (about 80 %) but might instead be a signature produced by low relative humidity in the dry spring (about 60 %) under a slow turnover rate of the surface water reservoir (Figure 1b). Additionally, the fact that the isotopic composition of Hailan River water does not fall on the extrapolated LEL of peatland water on the $\delta^2H$–$\delta^{18}O$ biplot indicates the separation of the peatland water balance from catchment runoff, further supporting the rain-fed nature of the site (Figure 6d).

**Comparisons with other European and North American sites**

In the subsections above, we show that there are different spatial patterns of isotopic variability in water at the peatland surface among different hydrogenetic types of peatlands within the same region of Northeast China, including a pristine sloping poor fen, a partially drained horizontal poor fen, and a sloping bog with pool patterning. We discuss how these differences reflect site-specific hydrological conditions and processes related to water sources, turnover and flow patterns. However, when placing our new findings in the context of existing literature, we find that these three sites are distinct from previously studied northern peatlands in Europe and North America in that our sites exhibit somewhat narrow ranges of site-specific variability in peatland water $\delta^{18}O$—no more than 2.5 ‰ in multiple surveys after excluding the agricultural pond at Jinchuan peatland (Figure 9). Supported by the results of model sensitivity analysis that allows for a quantitative understanding of the effects of various model variables (Figure 7b), we here seek to conduct further comparative analyses between our sites and previously studied well-characterised European and North American sites under similar settings, in order to explore the factors accounting for such regional differences.

Unlike Hani peatland that shows a very small (< 2 ‰) range of $\delta^{18}O$ variability, the evaporation-driven increase in peatland water $\delta^{18}O$ at a large bog-fen complex adjacent to McClelland Lake, Canada, is as high as 5 ‰ (around 7 ‰ across all samples) and occurs gradually along a sampled transect (Gibson *et al.* 2022; Figure 9). This site is comparable to Hani peatland in terms of catchment setting, with both peatlands showing progressive evaporation-induced isotopic enrichment downslope. Based on the sensitivity analysis, we suggest that the large-magnitude gradual increase in peatland water $\delta^{18}O$ at the McClelland Lake site may result from the large size and shallow slope of the peatland complex itself (30 $km^2$ with surface flow over a distance of about

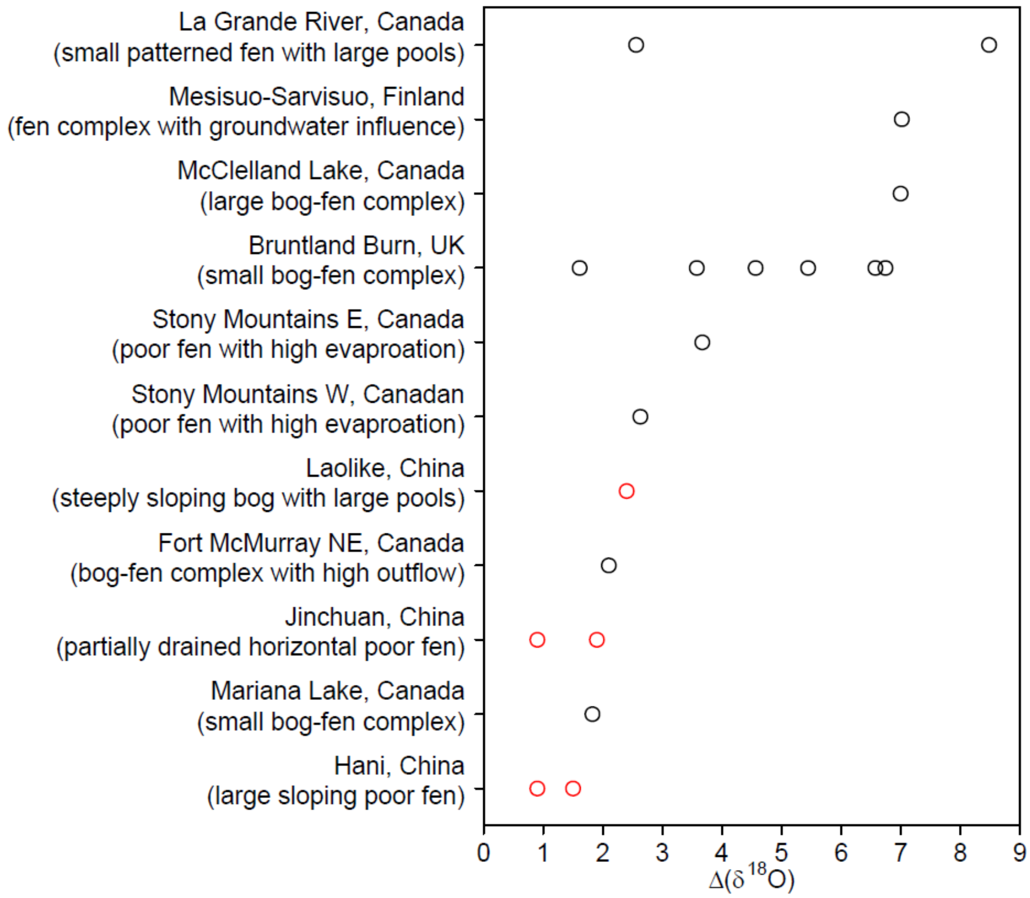


Figure 9. The range of $\delta^{18}O$ variability in water at the peatland surface reported from different peatlands in this study (red symbols) and the literature. For some sites, data were collected during multiple campaigns in different seasons and their ranges are plotted individually for each campaign. For Jinchuan peatland, the data collected from the agricultural pond are excluded. The references for literature data are: (1) La Grande River (Carrer *et al.* 2016); (2) Mesisuo-Sarvisuo (Isokangas *et al.* 2017); (3) McClelland Lake (Gibson *et al.* 2022); (4) Bruntland Burn (Sprenger *et al.* 2017); (5) Stony Mountains and Fort McMurray (Whitfield *et al.* 2010); and (6) Mariana Lake (Graham *et al.* 2016). For Stony Mountains, Fort McMurray and Mariana Lake (all located in Alberta, Canada), the ranges of surface water $\delta^{18}O$ are back-calculated from reported deuterium excess data by assuming a slope of 5 for local evaporation lines based on the McClelland Lake data.

8 km and an elevation drop of <10 m; Gibson *et al.* 2022), which amplifies the total magnitude of evaporative enrichment, and from high moss coverage promoting evaporation over transpiration (Admiral & Lafleur 2007, Gibson *et al.* 2022), which prevents the aforementioned plateau behaviour (Figure 7b).

The small Bruntland Burn bog-fen complex in the UK shows a range of $\delta^{18}O$ variability in water at the peatland surface of up to 6 ‰ in dry late summeracross downslope transect of only 100 m from the margin to the central open field (Sprenger *et al.* 2017; Figure 9). This site is comparable to Jinchuan peatland in terms of its similarly small size and strongly evaporative enrichment signal at the most-exposed central locations. Likewise, the groundwater-fed Mesisuo-Sarvisuo fen complex in Finland has spatially heterogeneous variations in peatland water $\delta^{18}O$ with a range of about 7 ‰, previously interpreted as reflecting a mosaic of groundwater-recharged zones and strong evaporation zones due to poor hydrological connectivity within the peatland (Isokangas *et al.* 2017; Figure 9). This site is also potentially comparable to Jinchuan peatland for their similar groundwater influences causing isotopic heterogeneity and similarly low hydraulic conductivity (on the scale of $10^{-6}$–$10^{-4}$ m $s^{-1}$ at 10 cm depth; Isokangas *et al.* 2017). To explain the much smaller $\delta^{18}O$ range encountered at Jinchuan peatland compared to these two sites, we suggest that, in addition to the high moss coverage at the Bruntland Burn bog-fen complex favouring fractionating evaporation over non-fractionating transpiration, regional climatic differences between Jinchuan peatland and the European sites may be a plausible factor. In the wet, monsoon-affected climate of Northeast China, the substantial precipitation input (on average, >150 mm $month^{-1}$ precipitation and > 80 % relative humidity in summer; Figure 1b) into peatland catchments is likely to accelerate the turnover of surface water reservoir and limit the extent of strongly enriched isotopic signatures, despite the fact that the human-made drainage may have reduced horizontal flows.

A small patterned fen with large pools near the La Grande River in Quebec, Canada, has a range of $\delta^{18}O$ variability across successive pools of about 8 ‰ in dry early summer (Carrer *et al.* 2016; Figure 9). This site is comparable to Laolike peatland for their similarly small sizes and the development of pool patterning. Although Laolike peatland shows the largest magnitude of isotopic variability among the three sites investigated in this study, it still exhibits a considerably smaller range than that observed at the patterned fen in Canada. This difference, once again, may be attributed primarily to regional climatic differences: the monsoon climate in Northeast China accelerates surface water turnover, thereby limiting the extent of strongly enriched isotopic signatures, whereas under the climatic and hydrological conditions of eastern Canada, peatland water tends to have a slower turnover during dry periods.

**Implications for water isotope techniques in studying peatland hydrology**

Using three peatlands of different hydrogenetic types from the same region as examples, the major implication of this study is that spatial isotope data surveyed at the peatland surface within a single site provide a simple, fast, low-cost and effective means of mapping the heterogeneity of water sources, assessing the timescale of water turnover, delineating possible water flow patterns across the site, and quantifying hydrological differences between sites and regions. This information is particularly relevant for understanding the ecosystem functions of peatlands, including biodiversity patterns (Oloo *et al.* 2016, Quenta *et al.* 2016, Schulte *et al.* 2019), the regulation of water flows in response to flooding and droughts (Goodbrand *et al.* 2019, Karimi *et al.* 2023), the efficiency of nutrient and pollutant transformation (Ronkanen & Kløve 2007, 2008; Graham *et al.* 2016), and the accumulation of key chemical compounds that influence peatland carbon sinks (Morris & Waddington 2011, Hribljan *et al.* 2014).

Additionally, the capability of model simulations to reproduce the patterns observed in field data indicates that a combined data-model approach has the potential to quantify hydrological processes, such as the relative contributions of surface evaporation and plant transpiration to evapotranspiration fluxes in peatland ecosystems if other variables are well constrained. Evapotranspiration partitioning is perhaps the least understood ecosystem process, yet it crucially controls how the peatland water budget responds to climate warming (Admiral *et al.* 2006, Admiral & Lafleur 2007, Wei *et al.* 2017, Helbig *et al.* 2020). Finally, this study also shows that the isotopic relationship between peatland water and adjacent river water is useful for identifying rain-fed and runoff-fed peatlands within a catchment basin. Therefore, such data can provide direct guidance for water resource and ecosystem management or improve the representation of individual peatlands in large-scale integrated hydrological models (Brooks *et al.* 2018, Rosa *et al.* 2018, Cooper *et al.* 2019, Wu *et al.* 2020).

While our research so far provides a case study and a preliminary framework for using the spatial pattern of water isotope ratios to investigate peatland hydrology, several developments could further enhance future research, including:

(1) conducting repeated sampling in different seasons and years to document temporal changes in peatland isotope hydrology (Sprenger *et al.* 2017, Stelling *et al.* 2021);

(2) increasing the spatial coverage and resolution of site-specific sampling;

(3) examining the depth profile of water isotope ratios, which may reveal the vertical pattern of groundwater flows (Levy *et al.* 2014);

(4) supporting the analysis with isotopic measurements of local precipitation, monitoring of the water table and collection of other environmental data (Graham *et al.* 2016); and

(5) improving the mechanistic model by incorporating other hydrological processes such as vertical flows and groundwater-surface-water exchange (Levy *et al.* 2014).

## ACKNOWLEDGEMENTS

We thank Kun Zhang, Yueyan Jiang, Yuwen Fu, Qiulei Yan and Yingfan Xia for assistance with fieldwork. This research was supported by the National Natural Science Foundation of China (42201167, 42494822), Fundamental Research Funds for the Central Universities (2412023YQ006, 135112004), Natural Science Foundation of Jilin Province (20230101077JC) and Environmental Protection Key Laboratory of Wetland Ecology and Vegetation Restoration Open Fund.

## AUTHOR CONTRIBUTIONS

ZX and CZ designed the project and secured the funding. ZX led the fieldwork and laboratory analysis. ZX and YLiu analysed the results and wrote the manuscript. CZ, YLi, and ZY contributed to the data interpretation. ZY provided the resources and supervised the project.

## REFERENCES

Admiral, S.W., Lafleur, P.M. (2007) Modelling of latent heat partitioning at a bog peatland. *Agricultural and Forest Meteorology*, 144(3), 213–229.

Admiral S.W., Lafleur P.M., Roulet N.T. (2006) Controls on latent heat flux and energy partitioning at a peat bog in eastern Canada. *Agricultural and Forest Meteorology*, 140(1), 308–321.

Arsenault, J., Talbot, J., Moore, T.R., Beauvais, M.-P., Franssen, J., Roulet, N.T. (2019) The spatial heterogeneity of vegetation, hydrology and water chemistry in a peatland with open-water pools. *Ecosystems*, 22(6), 1352–1367.

Baird, A.J., Eades, P.A., Surridge, B.W.J. (2008) The hydraulic structure of a raised bog and its implications for ecohydrological modelling of bog development. *Ecohydrology*, 1, 289–298.

Bao, K., Yu, X., Jia, L., Wang, G. (2010) Recent carbon accumulation in Changbai Mountain peatlands, Northeast China. *Mountain Research and Development*, 30(1), 33–41.

Beckwith, C.W., Baird, A.J., Heathwaite, A.L. (2003) Anisotropy and depth-related heterogeneity of hydraulic conductivity in a bog peat. II: Modelling the effects on groundwater flow. *Hydrological Processes*, 17(1), 103–113.

Bootsma, A., Elshehawi, S., Grootjans, A., Grundling, P.-L., Khosa, S., Butler, M., Brown, L., Schot, P. (2019) Anthropogenic disturbances of natural ecohydrological processes in the Matlabas mountain mire, South Africa. *South African Journal of Science*, 115(5–6), 1–9.

Brooks, J.R., Mushet, D.M., Vanderhoof, M.K., Leibowitz, S.G., Christensen, J.R., Neff, B.P., Rosenberry, D.O., Rugh, W.D., Alexander, L.C. (2018) Estimating wetland connectivity to streams in the prairie pothole region: An isotopic and remote sensing approach. *Water Resources Research*, 54(2), 955–977.

Carrer, G.E., Rousseau, A.N., Jutras, S., Fossey, M. (2016) Assessment of the impact of pools on the water isotopic signature of a boreal patterned peatland. *Hydrological Processes*, 30(8), 1292–1307.

Chamberlain, C.P., Winnick, M.J., Mix, H.T., Chamberlain, S.D., Maher, K. (2014) The impact of neogene grassland expansion and aridification on the isotopic composition of continental precipitation. *Global Biogeochemical Cycles*, 28(9), 992–1004.

Chapman, J.B., Lewis, B., Litus, G. (2003) Chemical and isotopic evaluation of water sources to the fens of South Park, Colorado. *Environmental Geology*, 43(5), 533–545.

Chen, X., Mallik, A.U., Yu, Z., Wang, Z., Wang, S., Dong, Y., Zhang, M.-M., Bu, Z.-J. (2024) Drainage-driven loss of carbon sequestration of a temperate peatland in Northeast China. *Ecosystems*, 27, 207–221.

Cooper, D.J., Sueltenfuss, J., Oyague, E., Yager, K., Slayback, D., Caballero, E.M.C., Argollo, J., Mark, B.G. (2019) Drivers of peatland water table dynamics in the central Andes, Bolivia and Peru. *Hydrological Processes*, 33(13), 1913–1925.

Couwenberg, J., Joosten, H. (2005) Self-organization in raised bog patterning: The origin of microtope zonation and mesotope diversity. *Journal of Ecology*, 93(6), 1238–1248.

Daley, T.J., Barber, K.E., Street-Perrott, F.A., Loader, N.J., Marshall, J.D., Crowley, S.F., Fisher, E.H. (2010) Holocene climate variability revealed by oxygen isotope analysis of *Sphagnum* cellulose from Walton Moss, northern England. *Quaternary Science Reviews*, 29(13), 1590–1601.

Devito, K.J., Waddington, J.M., Branfireun, B.A. (1997) Flow reversals in peatlands influenced by local groundwater systems. *Hydrological Processes*, 11(1), 103–110.

Dong, Y., Li, H., He, H., Wang, S. (2021) Holocene peatland development, carbon accumulation and its response to climate forcing and local conditions in Laolike peatland, northeast China. *Quaternary Science Reviews*, 268, 107124, 12 pp.

Eppinga, M.B., de Ruiter P.C., Wassen, M.J., Rietkerk, M. (2009) Nutrients and hydrology indicate the driving mechanisms of peatland surface patterning. *The American Naturalist*, 173(6), 803–818.

Evans, M.G., Burt, T.P., Holden, J., Adamson, J.K. (1999) Runoff generation and water table fluctuations in blanket peat: Evidence from UK data spanning the dry summer of 1995. *Journal of Hydrology*, 221(3), 141–160.

Fluet-Chouinard, E., Stocker, B.D., Zhang, Z., Malhotra, A. and 17 others (2023) Extensive global wetland loss over the past three centuries. *Nature*, 614(7947), 281–286.

Fraser, C.J.D., Roulet, N.T., Lafleur, M. (2001) Groundwater flow patterns in a large peatland. *Journal of Hydrology*, 246(1), 142–154.

Gat, J.R. (1996) Oxygen and hydrogen isotopes in the hydrologic cycle. *Annual Review of Earth and Planetary Sciences*, 24(1), 225–262.

Gibson, J.J., Edwards, T.W.D. (2002) Regional water balance trends and evaporation-transpiration partitioning from a stable isotope survey of lakes in northern Canada. *Global Biogeochemical Cycles*, 16(2), 1026, 18 pp.

Gibson, J.J., Birks, S.J., Yi, Y. (2016) Stable isotope mass balance of lakes: A contemporary perspective. *Quaternary Science Reviews*, 131, 316–328.

Gibson, J.J., Birks, S.J., Castrillon-Munoz, F., House, M., Vitt, D., Fan, X. (2022) Moss cellulose $^{18}O$ applied to reconstruct past changes in water balance of a boreal wetland complex, northeastern Alberta. *CATENA*, 213, 106116, 11 pp.

Goodbrand, A., Westbrook, C.J., van der Kamp, G. (2019) Hydrological functions of a peatland in a Boreal Plains catchment. *Hydrological Processes*, 33(4), 562–574.

Graham, J.A., Hartsock, J.A., Vitt, D.H., Wieder, R.K., Gibson, J.J. (2016) Linkages between spatio-temporal patterns of environmental factors and distribution of plant assemblages across a boreal peatland complex. *Boreas*, 45(2), 207–219.

Helbig, M., Waddington, J.M., Alekseychik, P., Amiro B.D. and 55 others (2020) Increasing contribution of peatlands to boreal evapotranspiration in a warming climate. *Nature Climate Change*, 10(6), 555–560.

Hokanson, K.J., Peterson, E.S., Devito, K.J., Mendoza, C.A. (2020) Forestland-peatland hydrologic connectivity in water-limited environments: Hydraulic gradients often oppose topography. *Environmental Research Letters*, 15(3), 034021, 12 pp.

Holden, J. (2005) Peatland hydrology and carbon release: why small-scale process matters. *Philosophical Transactions of the Royal Society A: Mathematical, Physical and Engineering Sciences*, 363(1837), 2891–2913.

Holden, J., Evans, M.G., Burt, T.P., Horton, M. (2006) Impact of land drainage on peatland hydrology. *Journal of Environmental Quality*, 35(5), 1764–1778.

Hong, Y.T., Jiang, H.B., Liu, T.S., Zhou, L.P., Beer, J., Li, H.D., Leng, X.T., Hong, B., Qin, X.G. (2000) Response of climate to solar forcing recorded in a 6000-year $\delta^{18}O$ time-series of Chinese peat cellulose. *The Holocene*, 10(1), 1–7.

Hribljan, J.A., Kane, E.S., Pypker, T.G., Chimner, R.A. (2014) The effect of long-term water table manipulations on dissolved organic carbon dynamics in a poor fen peatland. *Journal of Geophysical Research: Biogeosciences*, 119(4), 577–595.

Isokangas, E., Rossi, P.M., Ronkanen, A.-K., Marttila, H., Rozanski, K., Kløve, B. (2017) Quantifying spatial groundwater dependence in peatlands through a distributed isotope mass balance approach. *Water Resources Research*, 53(3), 2524–2541.

Joosten, H., Clarke, D. (2002) *Wise Use of Mires and Peatlands - Background and Principles including a Framework for Decision-Making*. International Mire Conservation Group and International Peat Society, Saarijärvi, Finland, 24–44.

Karimi, S., Leach, J., Karlsen, R.H., Seibert, J., Bishop, K., Laudon, H. (2023) Local- and network-scale influence of peatlands on boreal catchment response to rainfall events. *Hydrological Processes*, 37(10), e14998, 17 pp.

Keimowitz, A.R., Parisio, S., Adams, M.S., Interlichia, K., Halton, C., Kroenke, S., Hubert, A. (2013) Identification of ombrotrophic bogs in the Catskill Mountains, NY by geochemical and isotopic methods. *Wetlands*, 33(2), 355–364.

Levy, Z.F., Siegel, D.I., Dasgupta, S.S., Glaser, P.H., Welker, J.M. (2014) Stable isotopes of water show deep seasonal recharge in northern bogs and fens. *Hydrological Processes*, 28(18), 4938–4952.

Li, Y., Yu, Z., Wang, M., Li, H., Sun, J., Wang, S. (2024) Control of local topography and surface patterning on the formation and stability of a slope permafrost peatland at 4800-m elevation on the central Qinghai-Tibetan Plateau. *Ecological Indicators*, 158, 111475, 15 pp.

Li, M., Xia, Z., Li, Y., Dong, Y., Yu, Z. (2025) Simulating carbon accumulation of rain-fed peatlands in the East Asian monsoon region using the DigiBog model: Parameter sensitivity and climate response mechanisms. *Quaternary Sciences*, 45(3), 789–805 (in Chinese with English abstract).

Liu, H., Price, J., Rezanezhad, F., Lennartz, B. (2020) Centennial-scale shifts in hydrophysical properties of peat induced by drainage. *Water Resources Research*, 56(10), e2020WR027538, 14 pp.

Ma, L., He, C., Bian, H., Sheng, L. (2016) MIKE SHE modeling of ecohydrological processes: Merits, applications, and challenges. *Ecological Engineering*, 96, 137–149.

Ma, L. (2020) *Study on Eco-hydrology and Ecosystem Health Diagnosis of Peatland in Northeast China*. PhD dissertation, Northeast Normal University, Changchun, China, 166 pp. (in Chinese with English abstract).

Maselli, O.J., Fritzsche, D., Layman, L., McConnell, J.R., Meyer, H. (2013) Comparison of water isotope-ratio determinations using two cavity ring-down instruments and classical mass spectrometry in continuous ice-core analysis. *Isotopes in Environmental and Health Studies*, 49(3), 387–398.

Mathieu, R., Bariac, T. (1996) A numerical model for the simulation of stable isotope profiles in drying soils. *Journal of Geophysical Research*, 101(D7), 12685–12696.

Morris, P.J., Waddington, J.M. (2011) Groundwater residence time distributions in peatlands: Implications for peat decomposition and accumulation. *Water Resources Research*, 47, W02511, 12 pp.

Morris, P.J., Baird, A.J., Eades, P.A., Surridge, B.W.J. (2019) Controls on near-surface hydraulic conductivity in a raised bog. *Water Resources Research*, 55, 1531–1543.

Muhic, F., Ala-Aho, P., Noor, K., Welker, J.M., Klöve, B., Marttila, H. (2023) Flushing or mixing? Stable water isotopes reveal differences in arctic forest and peatland soil water seasonality. *Hydrological Processes*, 37(1), e14811, 22 pp.

Nichols, J., Booth, R.K., Jackson, S.T., Pendall, E.G., Huang, Y. (2010) Differential hydrogen isotopic ratios of *Sphagnum* and vascular plant biomarkers in ombrotrophic peatlands as a quantitative proxy for precipitation-evaporation balance. *Geochimica et Cosmochimica Acta*, 74(4), 1407–1416.

Oloo, F., Valverde, A., Quiroga, M.V., Vikram, S., Cowan, D., Mataloni, G. (2016) Habitat heterogeneity and connectivity shape microbial communities in South American peatlands. *Scientific Reports*, 6(1), 25712, 8 pp.

Prévost M., Plamondon A.P., Belleau P. (1999) Effects of drainage of a forested peatland on water quality and quantity. *Journal of Hydrology*, 214(1), 130–143.

Price, J.S., Maloney, D.A. (1994) Hydrology of a patterned bog-fen complex in southeastern Labrador, Canada. *Nordic Hydrology*, 25(5), 313–330.

Quenta, E., Molina-Rodriguez, J., Gonzales, K., Rebaudo, F., Casas, J., Jacobsen, D., Dangles, O. (2016) Direct and indirect effects of glaciers on aquatic biodiversity in high Andean peatlands. *Global Change Biology*, 22(9), 3196–3205.

Ronkanen, A.-K., Kløve, B. (2007) Use of stabile isotopes and tracers to detect preferential flow patterns in a peatland treating municipal wastewater. *Journal of Hydrology*, 347(3), 418–429.

Ronkanen, A.-K., Kløve, B. (2008) Hydraulics and flow modelling of water treatment wetlands constructed on peatlands in Northern Finland. *Water Research*, 42(14), 3826–3836.

Rosa, E., Dallaire, P.-L., Nadeau, S., Cloutier, V., Veillette, J., van Bellen, S., Larocque, M. (2018) A graphical approach for documenting peatland hydrodiversity and orienting land management strategies. *Hydrological Processes*, 32(7), 873–890.

Runkle, B.R.K., Wille, C., Gažovič, M., Wilmking, M., Kutzbach, L. (2014) The surface energy balance and its drivers in a boreal peatland fen of northwestern Russia. *Journal of Hydrology*, 511, 359–373.

Rydin, H., Jeglum, J.K. (2013) *The Biology of*

*Peatlands*. Second edition, Oxford University Press, Oxford UK, 1–20 and 199–229.

Schröder, C., Thiele, A., Wang, S., Bu, Z., Joosten, H. (2007) Hani-mire: A percolation mire in north-east China. *Peatlands International*, 2, 21–24.

Schulte, M.L., McLaughlin, D.L., Wurster, F.C., Balentine, K., Speiran, G.K., Aust, W.M., Stewart, R.D., Varner, J.M., Jones, C.N. (2019) Linking ecosystem function and hydrologic regime to inform restoration of a forested peatland. *Journal of Environmental Management*, 233, 342–351.

Shi, F., Rao, Z., Cao, J., Huang, C., Wu, D., Yang, W., Sun, W. (2019) Meltwater is the dominant water source controlling α-cellulose $\delta^{18}O$ in a vascular-plant-dominated alpine peatland in the Altai Mountains, Central Asia. *Journal of Hydrology*, 572, 192–205.

Sprenger, M., Tetzlaff, D., Tunaley, C., Dick, J., Soulsby, C. (2017) Evaporation fractionation in a peatland drainage network affects stream water isotope composition. *Water Resources Research*, 53(1), 851–866.

Stelling, J.M., Sebestyen, S.D., Griffiths, N.A., Mitchell, C.P.J., Green, M.B. (2021) The stable isotopes of natural waters at the Marcell Experimental Forest. *Hydrological Processes*, 35(10), e14336, 9 pp.

Sun, J.-J., Li, H.-C., Wang, J., Zhao, H.-Y., Wang, S.-Z., Li, H.-K., Yang, Q.-N., Chou, C.-Y., Kashyap, S. (2019) Study of Jinchuan Mire in NE China II: Peatland development, carbon accumulation and climate change during the past 1000 years. *Quaternary International*, 528, 18–29.

Swanson, D.K., Grigal, D.F. (1988) A simulation model of mire patterning. *Oikos*, 53(3), 309–314.

Tan, F. (2012) *Study on the Effects of Peat Properties on Hydrological Process in Jinchuan Wetland*. MSc thesis, Northeast Normal University, Changchun, China, 40 pp. (in Chinese with English abstract).

UNEP (2022) *Global Peatlands Assessment – The State of the World's Peatlands: Evidence for Action Toward the Conservation, Restoration, and Sustainable Management of Peatlands. Main Report*. United Nations Environment Programme, Nairobi, Kenya, 425 pp.

van Loon, A.H., Schot, P.P., Griffioen, J., Bierkens, M.F.P., Batelaan, O., Wassen, M.J. (2009) Throughflow as a determining factor for habitat contiguity in a near-natural fen. *Journal of Hydrology*, 379(1–2), 30–40.

Vitt, D.H., Bayley, S.E., Jin, T.-L. (1995) Seasonal variation in water chemistry over a bog - rich fen gradient in Continental Western Canada. *Canadian Journal of Fisheries and Aquatic Sciences*, 52(3), 587–606.

Vystavna, Y., Harjung, A., Monteiro, L.R., Matiatos, I., Wassenaar, L.I. (2021) Stable isotopes in global lakes integrate catchment and climatic controls on evaporation. *Nature Communications*, 12(1), 7224, 7 pp.

Wang, M., Liu, H., Lennartz, B. (2021) Small-scale spatial variability of hydro-physical properties of natural and degraded peat soils. *Geoderma*, 399, 115123, 12 pp.

Wei, H., Wang, Z., Xu, X., Xu, Z., Wang, S. (2022) The effects of long-term drainage and short-term restoration on dissolved organic C concentrations and optical properties in the Baijianghe Peatland. *Hydrological Processes*, 36(12), e14786, 12 pp.

Wei, Z., Yoshimura, K., Wang, L., Miralles, D.G., Jasechko, S., Lee, X. (2017) Revisiting the contribution of transpiration to global terrestrial evapotranspiration. *Geophysical Research Letters*, 44(6), 2792–2801.

Whitfield, C.J., Aherne, J., Gibson, J.J., Seabert, T.A., Watmough, S.A. (2010) The controls on boreal peatland surface water chemistry in Northern Alberta, Canada. *Hydrological Processes*, 24(15), 2143–2155.

Winnick, M.J., Chamberlain, C.P., Caves, J.K., Welker, J.M. (2014) Quantifying the isotopic 'continental effect'. *Earth and Planetary Science Letters*, 406, 123–133.

Wu, J., Kutzbach, L., Jager, D., Wille, C., Wilmking, M. (2010) Evapotranspiration dynamics in a boreal peatland and its impact on the water and energy balance. *Journal of Geophysical Research*, 115, G04038, 18 pp.

Wu, Y., Zhang, G., Rousseau, A.N., Xu, Y.J., Foulon, É. (2020) On how wetlands can provide flood resilience in a large river basin: A case study in Nenjiang river Basin, China. *Journal of Hydrology*, 587, 125012, 13 pp.

Xia, Z., Winnick, M.J. (2021) The competing effects of terrestrial evapotranspiration and raindrop re-evaporation on the deuterium excess of continental precipitation. *Earth and Planetary Science Letters*, 572, 117120, 13 pp.

Xing, W., Bao, K., Gallego-Sala, A.V., Charman, D.J., Zhang, Z., Gao, C., Lu, X., Wang, G. (2015) Climate controls on carbon accumulation in peatlands of Northeast China. *Quaternary Science Reviews*, 115, 78–88.

Xu, Z., Wang, Y., Li, H., Dong, Y., Wang, Z., Liu, Z., Liu, S., Sun, D., Zhao, H., Wang, S. (2024) Soil moisture and bacterial carbon limitation regulate the soil organic carbon in mountain peatlands. *CATENA*, 234, 107610, 13 pp.

Young, D.M., Baird, A.J., Morris, P.J., Holden, J. (2017) Simulating the long-term impacts of drainage and restoration on the ecohydrology of peatlands. *Water Resources Research*, 53(8), 6510–6522.

Zanazzi, A., Mora, G. (2005) Paleoclimatic implications of the relationship between oxygen isotope ratios of moss cellulose and source water in wetlands of Lake Superior. *Chemical Geology*, 222(3), 281–291.

Zhang, M., Bu, Z., Jiang, M., Wang, S., Liu, S., Jin, Q., Shi, P. (2019) Mid-late Holocene maar lake - mire transition in northeast China triggered by hydroclimatic variability. *Quaternary Science Reviews*, 220, 215–229.

Zhang, Z., Cao, Y., Wang, T., Bambalov, N.N. (1997) Comparative study on origin and development feature of peat mire. *Journal of Northeast Normal University*, 1997(3), 88–96 (in Chinese with English abstract).

Zhao, Y., Yu, Z., Tang, Y., Li, H., Yang, B., Li, F., Zhao, W., Sun, J., Chen, J., Li, Q., Zhou, A. (2014) Peatland initiation and carbon accumulation in China over the last 50,000 years. *Earth-Science Reviews*, 128, 139–146.

Zhou, W., Zheng, Y., Meyers, P.A., Jull, A.J.T., Xie, S. (2010) Postglacial climate-change record in biomarker lipid compositions of the Hani peat sequence, Northeastern China. *Earth and Planetary Science Letters*, 294(1), 37–46.

*Submitted 26 Jan 2024, final revision 06 Apr 2025*
*Editor: Gerald Jurasinski*

---

Authors for correspondence:
Dr Zhengyu Xia, School of Geographical Sciences, Northeast Normal University, 5268 Renmin Street, Changchun, 130024, Jilin Province, P.R. China. Email: zhyxia@hotmail.com
Dr Zicheng Yu, School of Geographical Sciences, Northeast Normal University, 5268 Renmin Street, Changchun, 130024, Jilin Province, P.R. China. Email: yuzc315@nenu.edu.cn